

Effects of Carrier Cooling and Carrier Heating in Saturation Dynamics and Pulse Propagation Through Bulk Semiconductor Absorbers

Alexander V. Uskov, *Member, IEEE*, J. R. Karin, John E. Bowers, *Fellow, IEEE*,
John G. McInerney, *Member, IEEE*, and Jean Le Bihan, *Member, IEEE*

Abstract—Numerical modeling has shown that carrier cooling and carrier heating strongly influence saturation dynamics and pulse shaping in bulk semiconductor absorbers. With no electric field in the absorbing region, carrier cooling leads to strong additional fast saturation of absorption. The saturation causes a substantial decrease in the saturation energies for subpicosecond pulses in comparison with picosecond pulses. Comparison of bulk and quantum-well absorbers shows that fast saturation can be stronger in a bulk absorber, so bulk saturable absorbers may be interesting for usage in mode-locked solid-state lasers. Applying a nonzero electric field to a bulk absorber leads to strong carrier heating, which in turn suppresses absorption saturation. In this case, transition to absorption saturation involves new mechanisms such as screening of the electric field by photogenerated carriers, as well as carrier cooling due to carrier–phonon interaction and by generated cold carriers. Carrier heating by the electric field causes the saturation energy of the absorber to increase with the applied electric field. The increased saturation energy allows one to shorten high-energy picosecond and subpicosecond pulses without increasing the length of the saturable absorber, which could be useful for the generation of high energy pulses with mode-locked and *Q*-switched semiconductor lasers.

Index Terms—Carrier heating, intraband carrier dynamics, mode-locked lasers, saturable absorbers, semiconductor lasers.

I. INTRODUCTION

INTRABAND carrier kinetics in semiconductors has attracted much attention because of their importance in defining and limiting high-speed laser performance. A great deal of attention has focused on the effects of intraband carrier kinetics, namely on spectral hole burning and carrier heating in semiconductor amplifying media (see, for instance, [1]–[15] and references therein). In passively mode-locked and *Q*-switched semiconductor [16]–[19] and solid-state [20]–[21]

lasers, semiconductor saturable absorbers play a principal role governing pulse generation. Intraband carrier kinetics in semiconductor absorbers can strongly influence the absorption saturation dynamics, defining, in fact, the scenario of mode-locking and pulse generation [20]–[23]. It explains why in the last few years the dynamics of saturation in semiconductor absorbers, particularly the effects of intraband carrier kinetics on absorption, have been studied [21], [24]–[29] in the same detail as gain dynamics in amplifiers. Complicated saturation dynamics based on intraband carrier kinetics have been demonstrated for both bulk [24]–[26] and quantum-well (QW) [21], [24], [27], [28] saturable absorbers. Those studies demonstrated that various mechanisms influence absorption dynamics in semiconductors, including nonthermal energy distribution of photogenerated carriers (like spectral hole burning in amplifiers) [21], [24]–[27], carrier cooling and heating [24]–[27], quantum-confined Stark effect [28], and the dynamics of excitonic absorption [29]. All these mechanisms are related to *intraband* carrier kinetics—transport of carriers in both energy and real spaces within the same energy band—and their characteristic times are of picosecond and femtosecond time scales, much shorter than *interband* carrier relaxation times.

Femtosecond pump-probe experiments on reverse-biased *bulk* PIN heterostructure waveguide saturable absorbers and modeling of these experiments are described in [24]–[26]. Those studies showed that carrier heating due to the electric field is significant in such absorbers, and this heating together with the dynamics of the electric field can have a dominant influence on the absorption saturation dynamics in bulk absorbers. Carrier heating by the electric field is impossible in QW structures, where the electric field is normal to QW's in which carriers are confined. Thus, electric field carrier heating principally distinguishes the saturation dynamics in bulk and QW absorbers. The temperature of the carriers in the QW, generated during absorption of light, is lower than lattice temperature; these “cold” carriers lead to “fast” saturation of absorption in addition to “slow” saturation [21]–[23], [27]. The fast saturation disappears on a picosecond time scale due to heating of the cold carriers to the lattice temperature. In bulk absorbers, carrier heating suppresses saturation of absorption [25], [26].

In this paper, we study theoretically the effects of carrier cooling and heating on the saturation dynamics and pulse

Manuscript received March 17, 1998; revised July 23, 1998. The work of A. V. Uskov was supported by Ministère de l'Enseignement, de la Recherche et de la Technologie, and Centre International des Etudiants et Stagiaires.

A. V. Uskov was with the Ecole Nationale d'Ingenieurs de Brest, Technopole Brest-Iroise-CP15, 29608 Brest Cedex, France, on leave from Lebedev Physical Institute, 117924 Moscow, Russia.

J. R. Karin is with the Center for Quantized Electronic Structures, University of California, Santa Barbara, CA 93106-4170 USA.

J. E. Bowers is with the Department of Electrical and Computer Engineering, University of California, Santa Barbara, CA 93106-9560 USA.

J. G. McInerney is with the Department of Physics/Optronics Ireland, National University of Ireland, University College Cork, Cork, Ireland.

J. Le Bihan is with Ecole Nationale d'Ingenieurs de Brest, Technopole Brest-Iroise-CP15, 29608 Brest Cedex, France.

Publisher Item Identifier S 0018-9197(98)08082-8.

propagation through bulk semiconductor waveguide saturable absorbers. This work is based on an extension of the model for femtosecond saturation dynamics in bulk absorbers [26]. Some preliminary results of the study have been published in [30].

In this paper, we assume that the absorption coefficient depends only on the carrier densities in the conduction and valence bands, and on carrier energy distributions (i.e., in fact, on carrier temperatures). An increase in carrier temperature decreases the quantity of carriers that are in resonance with photons and can saturate absorption. Thus, an increase of carrier temperature suppresses saturation, and the absorption coefficient approaches its unsaturated value. Conversely, carrier cooling leads to an increase in absorption saturation. This simple picture is the basis of several earlier studies [4]–[7], [9]–[11], [13]–[15], [22]–[27]. In contrast to amplifiers and QW absorbers, in reverse-biased bulk absorbers the electric field in the absorbing region provides an additional source of carrier heating and can significantly affect the absorption dynamics.

In this paper, we demonstrate how carrier cooling and carrier heating influence saturation in semiconductor absorbers. In particular, in the absence of an electric field in a bulk absorber, carrier cooling can lead to a substantial decrease in the absorption saturation energy for subpicosecond pulses. As a result, longer absorbers are needed to shorten high-power subpicosecond pulses. We compare fast saturation due to carrier cooling in bulk and QW absorbers and show that the fast saturation in bulk absorbers can be stronger than in QW's, so bulk absorbers might be preferable, for instance, in solid-state lasers where mode-locking is based on fast absorption saturation [20], [21].

In a bulk absorber, an electric field leads to strong carrier heating and substantial suppression of absorption. In particular, the saturation energy increases with the electric field. With increased saturation energy, higher energy pulses can be shortened without increasing the absorber length. In bulk absorbers with nonzero electric field, saturation dynamics, including the transition from unsaturated absorption to strong saturation and even to gain, are affected by screening of the electric field, and by carrier cooling due to carrier–phonon interaction and generated cold carriers. Thus we can talk about new mechanisms of saturation and improved pulse shaping in bulk absorbers.

The paper is organized as follows. In Section II, we describe the model used in the numerical study. Numerical results are given and discussed in Section III. Section III-A considers the case of zero electric field; together with numerical results, we also describe an approximate theory of absorption saturation and compare bulk and QW absorbers. Section III-B is devoted to the case of nonzero electric field in a bulk absorber. Section IV summarizes and concludes the paper.

II. THEORETICAL MODEL

We consider the situation illustrated in Fig. 1(a). A light pulse is propagating through a semiconductor waveguide absorber in the z direction. The waveguide has a cross section A_g and length L . Its active layer is of thickness d and width

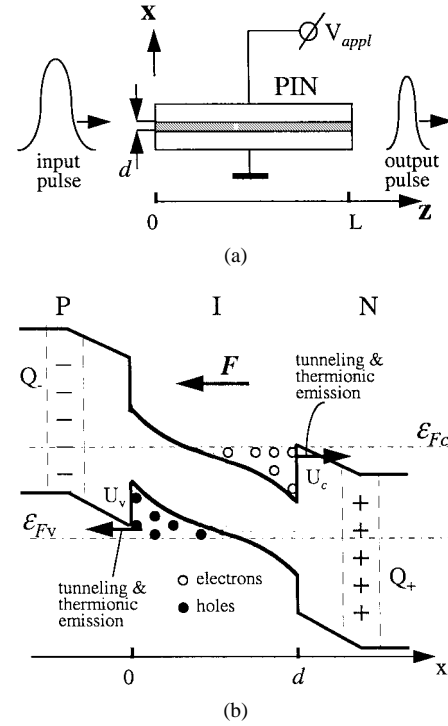


Fig. 1. (a) Illustration of the considered problem: the light pulse propagates through a PIN waveguide semiconductor absorber of length L and with active layer of thickness d . The reverse voltage V_{appl} is applied to the absorber. (b) Schematic band diagram of the absorber under consideration. Absorption takes place in the region $0 < x < d$. The field F is created by the charges Q_- and Q_+ of ionized impurities at the N-I and I-P junctions, respectively, and is due to the built-in voltage V_{bi} of the PIN structure and the externally applied voltage V_{appl} . Electrons (holes) leave the absorbing region through and over the barrier U_c (U_v) at the boundary $x = d$ ($x = 0$). The dash-dotted lines show the quasi-Fermi levels for electrons (ϵ_{F_c}) in the conduction band and for holes (ϵ_{F_v}) in the valence band.

w . The absorber is a PIN bulk heterostructure, so that d is the distance between two heterojunctions [see the energy band diagram of the device in Fig. 1(b)]. The charges Q_- and Q_+ of ionized impurities at the N-I and I-P junctions, respectively, create the electric field F in the absorbing region ($0 < x < d$). Before pulse injection into the device, the electric field $F = F_o$, where the initial field F_o is defined by the built-in voltage V_{bi} of the PIN structure and by the applied reverse bias voltage V_{appl} . The voltage V_{bi} can be ~ 1 V, so even in the absence of an applied voltage the initial field can be $F_o \sim 10^7$ V/m at $d \sim 100$ nm. As the light pulse generates carriers in the absorbing region, some of the carriers are transported to the heterojunctions and neutralize the charges Q_- and Q_+ , thereby changing, at least in part, the field F in the absorbing region.

Pulse propagation through the semiconductor waveguide absorber can be modeled with the propagation equation for the photon densities $S(z, t)$

$$\frac{\partial S}{\partial t} + v_g \frac{\partial S}{\partial z} = -\Gamma v_g \bar{\alpha}(z, t) \cdot S \quad (1)$$

where $\Gamma = wd/A_g$ is the confinement factor, v_g the group velocity, and $\bar{\alpha}(z, t)$ the absorption coefficient averaged over

the thickness d of the absorbing region (see Fig. 1)

$$\bar{\alpha}(z, t) = \frac{1}{d} \int_0^d dx \alpha(z, x, t). \quad (2)$$

The absorption coefficient $\alpha(z, x, t)$ at the point with coordinates x and z is defined by the energy distributions of carriers at this point. Let us note that because we concentrate on the propagation of picosecond pulses through relatively short ($\sim 50 \mu\text{m}$) absorbers, we have neglected any dispersion effects in the propagation equation (1). For shorter pulses (with duration ~ 100 fs) and for longer propagation distances (for instance, through an absorber in a cavity), the effects of dispersion can be important [31]. To describe the absorption dynamics, generally speaking, one has to solve the Boltzmann equation for carrier transport across the device in strong electric fields, together with the Poisson equation for the electric field in the absorbing region of the device. In order to avoid this very complicated problem, we restrict ourselves to the propagation of picosecond pulses, which greatly simplifies the problem. First, because intraband relaxation times (~ 100 fs) are much shorter than the pulse duration, we will assume that the carrier distribution at any point in the absorber at any moment in time is a Fermi distribution. In general, it is easy to introduce into the model nonthermal deviations from Fermi distributions, and the deviations will describe some effects in absorption dynamics similar to spectral hole burning in gain dynamics in amplifiers (see, for instance, [5], [6], [26]). The nonthermal effects can be important for femtosecond pulses with high photon densities; however, in this paper we will concentrate on carrier cooling and heating effects and neglect effects of nonthermal distributions.

Second, carrier transport times across the absorbing region in the presence of strong electric fields can be estimated as $\tau_{\text{tr}} = d/v_{\text{sat}}$, where v_{sat} is the saturated carrier drift velocity in high electric fields, $v_{\text{sat}} \sim 2 \cdot 10^5$ m/s [32]. For $d \sim 100$ nm, τ_{tr} is of subpicosecond time scale, which allows us to assume that on a picosecond time scale thermal equilibrium across the absorbing region exists at all times. This implies that carrier Fermi distributions are characterized by Fermi levels and temperatures which are independent of coordinate x across the absorbing region; only the electric potential varies with coordinate x . Thus the carrier distributions at the point x are given by

$$f_i(\varepsilon) = \left\{ 1 + \exp \left[\frac{\varepsilon + (\mp q)\varphi(x) - \varepsilon_{F_i}}{k_B T_i} \right] \right\}^{-1}, \quad i = c, v \quad (3)$$

where ε_{F_c} (ε_{F_v}) and T_c (T_v) are the Fermi level and temperature for the electrons (holes) in conduction (valence) band, ε is the kinetic energy of the carrier, $(\mp q)\varphi(x)$ is its potential energy, and $\varphi(x)$ is the potential which is defined by the electric field F and the distributions of photogenerated carriers in the absorbing region. The minus sign in (3) refers to the electrons ($i = c$), and the plus sign to the holes ($i = v$). The Fermi levels ε_{F_c} and ε_{F_v} , and the temperatures T_c and T_v can depend on the coordinate z along the absorber and on time t .

The absorption coefficient $\alpha(z, x, t)$ is expressed through the carrier distributions (3), and in the limit of nonhomo-

geneous broadening [33] can be written as

$$\alpha = \alpha_o(z, x, t) = \alpha_o \cdot (1 - f_c(\varepsilon_c^o) - f_v(\varepsilon_v^o)) \quad (4)$$

where α_o is the unsaturated absorption coefficient, ε_c^o (ε_v^o) is the energy of electrons (holes) in conduction (valence) band which are in resonance with photons of the energy $\hbar\omega_o$

$$\begin{aligned} \varepsilon_c^o &= (\hbar\omega_o - E_{\text{gap}}) \frac{m_v}{m_c + m_v} \\ \varepsilon_v^o &= (\hbar\omega_o - E_{\text{gap}}) \frac{m_c}{m_c + m_v} \end{aligned} \quad (5)$$

where E_{gap} is the energy bandgap in the absorbing region and m_c (m_v) is the electron (hole) mass.

The dynamics of the Fermi levels and temperatures, and accordingly, of the absorption (4), are given by the balance equations for carriers and their energy in the absorbing region

$$\frac{d\bar{n}_i}{dt} = S \cdot v_g \cdot \bar{\alpha}(z, t) - \frac{\bar{n}_i}{\tau_S} - R_n^i \quad (6)$$

$$\begin{aligned} \frac{d\bar{u}_i}{dt} &= S \cdot v_g \cdot \frac{1}{d} \int_0^d dx \cdot \alpha(z, x, t) \cdot [\varepsilon_i^o + (\mp q) \cdot \varphi(x)] \\ &\quad - \frac{\bar{u}_i}{\tau_S} - \frac{\bar{u}_i - \bar{u}_{Li}}{\tau_{ui}} - R_u^i, \quad i = c, v \end{aligned} \quad (7)$$

where \bar{n}_c and \bar{n}_v are, respectively, the electron and hole density, averaged across the absorbing region

$$\bar{n}_i = \frac{1}{d} \int_0^d dx \cdot n_i(x) \quad (8a)$$

$$n_i(x) = N_i \cdot F_{1/2} \left[\frac{\varepsilon_{F_i} - (\mp q)\varphi(x)}{k_B T_i} \right] \quad (8b)$$

and \bar{u}_c and \bar{u}_v are the averaged energy densities for electrons and holes, respectively:

$$\bar{u}_i(x) = \frac{1}{d} \int_0^d dx \cdot u_i(x) \quad (9a)$$

$$\begin{aligned} u_i(x) &= \frac{3}{2} k_B T_i \cdot N_i \cdot F_{3/2} \left[\frac{\varepsilon_{F_i} - (\mp q)\varphi(x)}{k_B T_i} \right] \\ &\quad + (\mp q) \cdot \varphi(x) \cdot n_i(x) \end{aligned} \quad (9b)$$

where N_i ($i = c, v$) is the effective density of states [32]

$$N_i = N_i(T_i) = 2 \cdot \left(\frac{m_i k_B T_i}{2\pi\hbar^2} \right)^{3/2}. \quad (10)$$

The first term in (9b) is the kinetic energy; the second term is the potential energy. The first terms in (6) and (7) are the pumping rates of carriers and energy into the absorbing region. Electrons (holes) are pumped by the pulse into the conduction (valence) band with the kinetic energy ε_c^o (ε_v^o) and the potential energy $(-q\varphi)$ [$+q\varphi$] [see (7)].

The second terms in (6) and (7) describe interband carrier relaxation. The third term in (7) describes energy relaxation due to carrier-phonon interactions [4], [5], [34]. \bar{u}_{Lc} (\bar{u}_{Lv}) is the energy density of electrons (holes) at the lattice temperature T_L and is calculated at the same averaged density \bar{n}_c (\bar{n}_v) and the same potential $\varphi(x)$ as in calculation of \bar{u}_c (\bar{u}_v). τ_{uc} (τ_{uv}) is the energy relaxation time for electron (hole) due to carrier-phonon interaction. $F_l(x)$ in (8b) and (9b) is the Fermi-Dirac integral of the order l .

R_n^i and R_u^i in (6) and (7) are the rates of removal of carriers and energy, respectively, from the absorbing region due to thermionic emission and tunneling through barriers at the heterojunctions [see Fig. 1(b)], and can be expressed in terms of the carrier distributions near the barriers (at $x = 0$ for holes, and at $x = d$ for electrons) and the transmission coefficients of these barriers:

$$R_n^i = \frac{m_i k_B T_i}{2\pi^2 \hbar^3} \int_0^\infty \int_0^\infty d\varepsilon_\perp d\varepsilon_{II} D_i(\varepsilon_\perp) \cdot \left\{ 1 + \exp \left[\frac{\varepsilon_\perp + \varepsilon_{II} + (\mp q)\varphi(x_i) - \varepsilon_{F_i}}{k_B T_i} \right] \right\}^{-1} \quad (11)$$

$$R_u^i = \frac{m_i k_B T_i}{2\pi^2 \hbar^3} \int_0^\infty \int_0^\infty d\varepsilon_\perp d\varepsilon_{II} \cdot (\varepsilon_\perp + \varepsilon_{II}) \cdot D_i(\varepsilon_\perp) \cdot \left\{ 1 + \exp \left[\frac{\varepsilon_\perp + \varepsilon_{II} + (\mp q)\varphi(x_i) - \varepsilon_{F_i}}{k_B T_i} \right] \right\}^{-1}, \quad (12)$$

$i = c, v.$

$D_i(\varepsilon_\perp)$ is the transmission coefficient for carriers impinging the barrier normally with the kinetic energy ε_\perp , $x_c = d$, and $x_v = 0$. In the model, we have assumed that $D_i = 1$ if the energy ε_\perp of the carrier is larger than the height U_i of the barrier [see Fig. 1(b)], $\varepsilon_\perp > U_i$ (thermionic emission). For $\varepsilon_\perp < U_i$ (tunneling), the coefficient is calculated assuming that the barrier has a triangular shape with the slope determined by the electric field F in the barrier (Fowler–Nordheim tunneling) [35].

The potential $\varphi(x)$ can be written as

$$\varphi(x) = F \cdot x + \tilde{\varphi}(x) \quad (13)$$

where the screening potential $\tilde{\varphi}(x)$ is calculated from the Poisson equation

$$\frac{\partial^2 \tilde{\varphi}}{\partial x^2} = \frac{q}{\varepsilon \varepsilon_0} [n_c(x) - n_v(x)] \quad (14)$$

with the boundary conditions

$$\tilde{\varphi}(x=0) = 0 \quad (14a)$$

$$\frac{\partial \tilde{\varphi}}{\partial x}(x=0) = -\frac{\partial \tilde{\varphi}}{\partial x}(x=d), \quad (14b)$$

In (14), ε_0 is the vacuum permittivity, and ε is the dielectric constant. The condition (14b) means that the screening electric field, which is created by the carrier distributions $n_c(x)$ and $n_v(x)$ in the absorbing region, has the same value, but the opposite directions at the boundaries $x = 0$ and $x = d$.

As mentioned above, the electric field F is created by the charges Q_- and Q_+ of ionized impurities. Due to thermionic emission and tunneling of photogenerated carriers from the absorbing region, the charges Q_- and Q_+ change, which lead to variations in the field F . Dynamics of the field F can be evaluated from

$$\frac{dF}{dt} = -\frac{q}{2\varepsilon \varepsilon_0} (R_c + R_v) - \frac{F - F_0}{\tau_{RC}}. \quad (15)$$

Detailed derivation of (15) (based on Kirchhoff laws) is given in [26]. The first term in (15) is due to thermionic emission and tunneling, and the second term describes the effect of the

external circuit on the recovery of the field. $\tau_{RC} = R_s C$ is the RC -time of the circuit, where R_s is the series resistance and C is the capacitance of the saturable absorber structure. Any RC -induced delay in removal of charge through the rest of the circuit results in a delay in the recovery of the field in the absorbing region.

Equations (1), (6), (7) along with (14) and (15) are used in this paper to study numerically picosecond pulse propagation through a semiconductor waveguide absorber. Note that at $\varphi = 0$ (6)–(9) are reduced to the usual models [4]–[7], [10], [13], [15] used for bulk semiconductor optical amplifiers. In [22], [23], and [27], the model of (6)–(7) with corresponding changes for the two-dimensional (2-D) case in (8) and (9) also has been used to describe the absorption dynamics in QW absorbers in modeling mode-locked lasers. In this case, photogenerated carriers are confined in the QW in the direction of the external field F , so the field is not able to heat the carriers in the QW. The influence of the field on carrier temperature dynamics can therefore be neglected, and the potential φ can be put to zero in (7) and (9b). In QW absorbers, the electric field only influences the tunneling rates from the QW. We consider the case of $\varphi = 0$ in Section III-A.

Thus, (6), (7) and (14), (15) can be considered a generalization of earlier models for the case of a nonzero electric field in the active region of the device.

III. NUMERICAL RESULTS AND DISCUSSION

The calculations have been done for a GaAs–GaAlAs structure. The effective masses of electrons and holes have been taken as 0.067 and 0.34, respectively. The values of barriers for electrons and holes at the boundaries of absorbing region ($x = 0, W$ [see Fig. 1(a)] have been assumed to be 0.38 and 0.25 eV, respectively. The energy bandgap in the absorbing region $E_{\text{gap}} = 1.48$ eV. The length L of the absorber is 50 μm . The thickness d of the absorbing region is 100 nm, and the width w is 3.5 μm . The confinement factor $\Gamma = 0.2$. The input pulse is assumed to be of Gaussian shape: $S = S_{\text{max}} \cdot \exp(-t^2/\tau_o^2)$ with the full-width at half-maximum (FWHM) $\tau_{\text{in}} = 2\sqrt{\ln 2} \cdot \tau_o$. The photon energy $\hbar\omega_o$ is 1.49 eV. The unsaturated absorption coefficient is assumed to be $\alpha_o = 1.3 \cdot 10^5 \text{ m}^{-1}$. The carrier relaxation time $\tau_S = 300$ ps. The characteristic RC time of the external circuit $\tau_{RC} = 50$ ps. The carrier energy relaxation times $\tau_{uc} = \tau_{uv} = 1$ ps [5], [7], [34]. Other parameters of the device and of the input pulse can be found in the next sections.

A. Neglecting Field Effects: Carrier Cooling

In this section we assume $\varphi = 0$ in (5)–(8) and neglect thermionic emission and tunneling ($R_n^i = 0, R_u^i = 0$). This case is interesting from several points of view. First, we can use this case as background in the description of electric field effects in bulk semiconductor absorbers. Second, as mentioned above, the equations for saturation dynamics in bulk absorbers in this zero-field case are similar to ones for QW absorbers, so the analysis can be useful for semiconductor and solid-state mode-locked and Q -switched lasers that use QW structures as saturable absorbers. Third, bulk semiconductor absorbers may

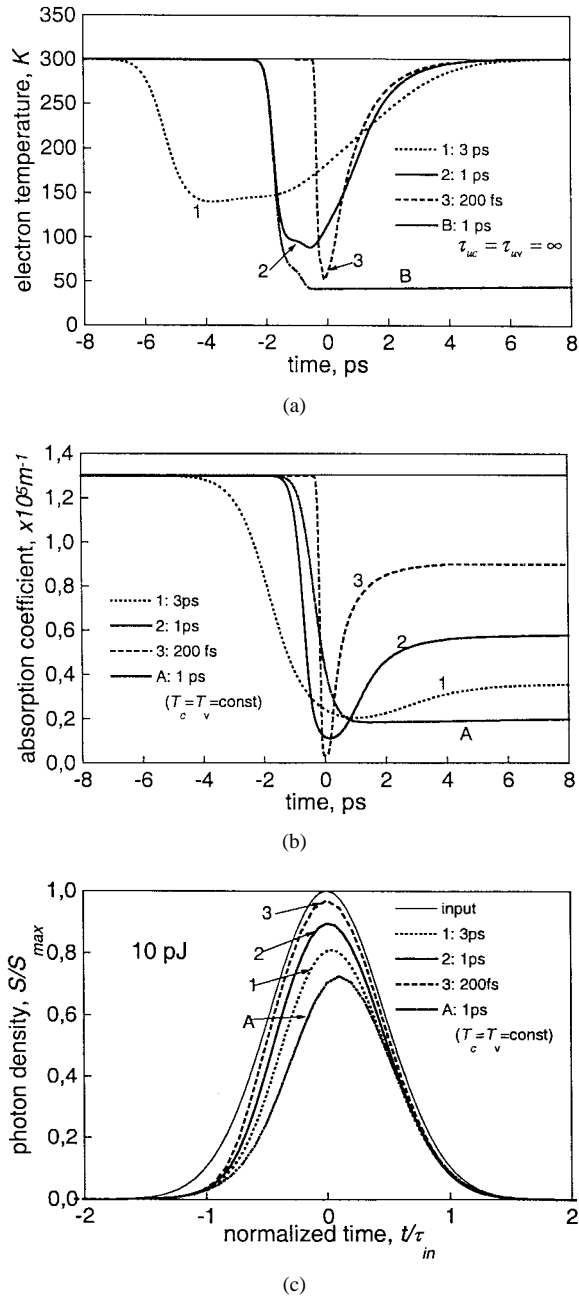


Fig. 2. (a) Calculated electron temperature dynamics, (b) absorption coefficient dynamics, and (c) output pulses for different pulse durations for an absorber with zero initial electric field ($F_o = 0$): dotted curves 1 for 3 ps; solid curves 2 for 1 ps; dashed curves 3 for 200 fs; curves A for 1 ps and $T_c = T_v = 300$ K; curves B for 1 ps and $\tau_{uc} = \tau_{uv} = \infty$. The thin solid curve in (c) is the input pulse. In (c), time and photon densities are normalized with the pulse duration τ_{in} and S_{max} , respectively, separately for each case of pulse duration τ_{in} . In all cases, the input pulse energy $E_{in} = 10$ pJ is assumed.

be interesting for application in solid-state lasers. Note that because there is no electric field in the structure, there is no carrier transport across the structure and therefore the model can also be used for subpicosecond pulses.

Fig. 2(a) shows electron temperature dynamics in the point $x = 40 \mu m$ in the absorber for the input pulse energy 10 pJ and different input pulsewidths (3 ps, 1 ps, and 200 fs). The hole temperature behaves similarly. Before the pulse, a small

quantity of carriers with the lattice temperature $T_L = 300$ K is assumed to be in the absorber. The pulse generates cold electrons with the energy $\varepsilon_c^o = 8.3$ meV [see (5)], so the temperature of electrons in the absorbing region decreases at first, and then it relaxes again to the lattice temperature due to electron-phonon interaction. Curve B in Fig. 2(a) shows temperature behavior if we neglect electron-phonon interaction [$\tau_{uc} = \tau_{uv} = \infty$ in (7)]. In this case, the electron temperature, which is established after the pulse, differs from the lattice temperature. From Fig. 2(a) we see that carrier cooling is stronger for shorter pulses (see curves 1–3), which is in agreement with the conclusion for amplifiers [7] that temperature dynamics are more important for shorter pulses, and for longer pulses can be neglected.

Fig. 2(b) shows the corresponding dynamics of the absorption coefficient. Curve A demonstrates absorption behavior when we neglect temperature dynamics ($T_c = T_v = 300$ K) for a pulse duration of 1 ps. We see that carrier cooling leads to stronger saturation (curve 2 versus curve A). In fact, the absorption saturates due to carriers generated by the pulse and due to their cooling in relation to the lattice temperature. Relaxation of carrier temperature to the lattice temperature leads to partial fast recovery of absorption. Further long recovery of absorption is defined by carrier lifetimes in the absorbing region. When tunneling and thermionic emission are neglected, the long recovery is characterized by the interband relaxation time $\tau_s = 300$ ps. The contribution of the fast recovery is more important for shorter pulses (see curve 3), and in this case the fast recovery is more pronounced. The same fast saturation due to carrier cooling takes place in QW saturable absorbers as well and could be responsible for mode-locking in solid-state lasers with semiconductor QW saturable absorbers [20], [21]. In [22] and [23], the fast saturation has been discussed as one of the possible mechanisms of mode-locking in QW semiconductor lasers.

Fig. 2(c) shows the input and output optical pulses. Pulse photon density and time in Fig. 2(c) are normalized with the input maximum photon density S_{max} , and the pulse duration τ_{in} , respectively, separately for each of the different input pulse durations. It allows us to compare pulse shaping for different input pulse durations. We see that carrier-temperature-induced absorption saturation strongly influences pulse shaping (compare curve 2 with curve A) where temperature effects are ignored. It demonstrates the necessity to take into account these effects for proper modeling of short-pulse semiconductor lasers. We also see that for the same input pulse energy shorter pulses experience less pulse shortening. This last fact is a consequence of the dependence of saturation energy on pulse duration due to the considered temperature effects. Shorter pulses have smaller saturation energy, so they saturate absorption much more easily than longer pulses, and therefore experience less pulse shortening.

The dependence of saturation energy on pulsewidth is seen from Fig. 3 where the absorber transmission E_{out}/E_{in} (E_{in} is the input pulse energy, E_{out} is the output pulse energy) is shown as a function of the input pulse energy E_{in} for different input pulse durations (curves 1–3). Curve A is obtained by neglecting temperature effects ($T_c = T_v = 300$ K) and

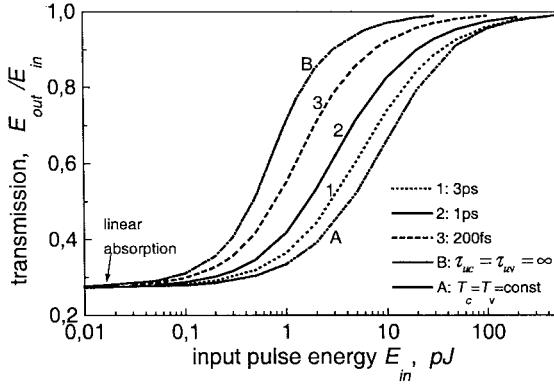


Fig. 3. Calculated dependence of the transmission E_{out}/E_{in} on the input pulse energy E_{in} for different pulse durations, for an absorber with zero initial electric field ($F_0 = 0$). Notations for the curves are the same as in Fig. 2.

does not depend, in fact, on pulse duration if we neglect carrier relaxation ($\tau_S = \infty$; see, for instance, [7], [36]). If we increase the pulse duration τ_{in} , so that temperature effects become negligible, the resulting transmission curves approach curve A. Curve B is obtained by neglecting electron–phonon interaction ($\tau_{uc} = \tau_{uv} = \infty$). This curve B is approached by the transmission curves if we decrease the input pulse duration τ_{in} . The importance of carrier cooling effects in absorption saturation by picosecond and subpicosecond pulses is obvious from Fig. 3. In fact, the saturation energy for long and short pulses can be different by one order of magnitude. The dependence of saturation dynamics on pulse duration is important for the design of short-pulse lasers which use saturable absorber pulse shaping. For shortening, the transmission coefficient must be far from its linear value (see Fig. 3) (otherwise the absorber will absorb the pulse linearly without shortening), and far from 1 [otherwise the pulse will be shortened only a little, as with the 200-fs pulse in Fig. 2(c)], i.e., a pulse with energy close to the saturation energy of the absorber is shortened most effectively. From Fig. 3, we can conclude that the modeled absorber will effectively shorten a pulse with a duration of 1 ps and energy of 1 pJ. In order to shorten stronger pulses of the same duration, we can use a longer absorber, or use a new approach to increase the saturation energy. One such approach is to apply an electric field across the absorbing region. This approach is discussed in Section III-B.

We note that in this paper we consider only temperature effects and neglect any effects of nonthermal carrier distributions in the absorbers. In fact, a nonthermal distribution (like spectral hole burning (SHB) in semiconductor optical amplifiers) does lead to an additional contribution to absorption saturation, the contribution being larger for shorter and stronger pulses. In particular, if SHB were included, the additional reduction in absorption due to the nonthermal distribution would change the curves in Fig. 3. Curve 3 (the 200-fs pulse) would change most substantially: most of this curve would move to the axis of the ordinate, so that the saturation energy ($E_{out}/E_{in} \sim 0.5$) decreases by 1.5–2 times. Curves 1 and 2 modify strongly only at large input energies E_{in} , so that the characteristic saturation energies for the 1- and 3-ps pulses do not change substantially.

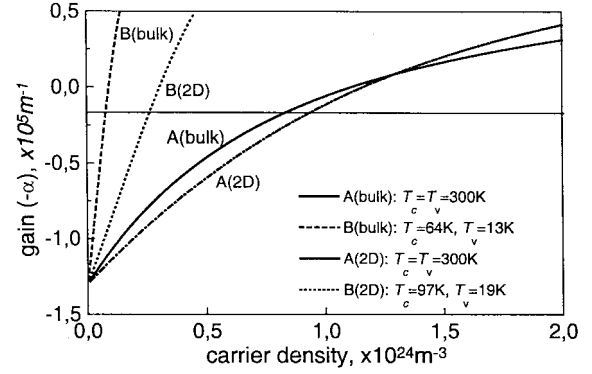


Fig. 4. Dependence of gain ($-\alpha$) on carrier density. Curve A(bulk) is for bulk absorber and $T_c = T_v = 300$ K, curve B(bulk) is for bulk absorber and $T_c = 64$ K, $T_v = 13$ K. Curve A(2D) is for QW absorber and $T_c = T_v = 300$ K, and curve B(2D) is for QW absorber and $T_c = 97$ K, $T_v = 19$ K. For additional explanation on curves B, see Section III-A.

It is also worth noting that the pulsewidth-dependent effects of carrier temperature on gain saturation in semiconductor optical amplifiers were experimentally identified in [5] and [6], and theoretically modeled in [7].

The two limit cases A and B in Figs. 2 and 3 can be analyzed and approximated as follows. The absorption coefficient (4) is a function of the carrier densities n_c and n_v , and carrier temperatures T_c and T_v :

$$\alpha = \alpha(n_c, n_v, T_c, T_v). \quad (16)$$

In the considered case of zero electric field, $n_c = n_v = n$. Assuming $T_c = T_v = T_L$ (curves A), we have that the absorption coefficient depends only on the carrier density n

$$\alpha = \alpha(n, n, T_L, T_L) = \alpha_A(n). \quad (17)$$

The dependence of the gain $g = -\alpha$ on the carrier density n for this case is shown in Fig. 4 with curve A (bulk). The dependence $\alpha = \alpha_A(n)$ is linear for small n and can be approximated as

$$\alpha = \alpha_o - \alpha_{nA} \cdot n. \quad (18)$$

The “differential absorption” α_{nA} can be found with (4)

$$\alpha_{nA} = \alpha_o \cdot \left(\frac{\exp(-\varepsilon_c^o/k_B T_L)}{N_c(T_L)} + \frac{\exp(-\varepsilon_v^o/k_B T_L)}{N_v(T_L)} \right). \quad (19)$$

In the case of short pulses ($\tau_{in} \ll \tau_{uc}, \tau_{uv}$), we can neglect carrier–phonon interaction. Then the temperatures T_c^o and T_v^o of generated electrons and holes, which are established as a result of carrier–carrier collisions, can be calculated from the energy balance equations

$$\varepsilon_c^o \cdot n = u_c(n, T_c^o), \quad \varepsilon_v^o \cdot n = u_v(n, T_v^o). \quad (20)$$

Here we have neglected any initial carriers in the absorber with temperature T_L before the arrival of the pulse. In general, the temperatures T_c^o and T_v^o depend on the density n of generated carriers. However, if we assume Boltzmann statistics, so that in the three-dimensional (3-D) case

$$u_i = \frac{3}{2} k_B T_i \cdot n_i \quad (21)$$

we obtain

$$T_i^o = \bar{T}_i^{\text{bulk}} = \frac{2\varepsilon_i^o}{3k_B}. \quad (22)$$

It is possible to show that the approximation with Boltzmann statistics leads to errors of no more than 10% in the calculation of temperatures for the considered range of carrier densities.

The absorption coefficient is then given as

$$\alpha = \alpha(n, n, \bar{T}_c^{\text{bulk}}, \bar{T}_v^{\text{bulk}}) = \alpha_B(n) \quad (23)$$

or

$$\alpha = \alpha_o - \alpha_{nB} \cdot n \quad (24)$$

where the “differential absorption” is

$$\alpha_{nB} = \alpha_o \cdot \left(\frac{\exp(-\varepsilon_c^o/k_B \bar{T}_c^{\text{bulk}})}{N_c(\bar{T}_c^{\text{bulk}})} + \frac{\exp(-\varepsilon_v^o/k_B \bar{T}_v^{\text{bulk}})}{N_v(\bar{T}_v^{\text{bulk}})} \right). \quad (25)$$

Curve B(bulk) in Fig. 4 shows the dependence of the gain on the carrier density for this case. In the considered case $\bar{T}_c^{\text{bulk}} = 64$ K, $\bar{T}_v^{\text{bulk}} = 13$ K. The dependences A(bulk) and B(bulk) can be used to calculate curves A and B in Figs. 2 and 3 for long and short pulses, respectively. We see that the difference between two curves A (bulk) and B(bulk) is very large. In particular, the differential absorptions α_{nA} and α_{nB} are different by one order of magnitude.

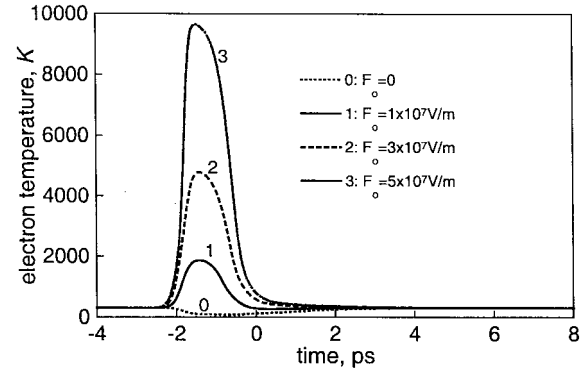
Curve A(2D) in Fig. 4 shows the gain dependence on the carrier density for the QW in the case when $T_c = T_v = 300$ K. Curve B(2D) gives the dependence when carrier-phonon interaction is negligible, the electron and hole temperatures in the QW being defined by the energies ε_c^o and ε_v^o of pumped electrons and carriers (2-D Boltzmann statistics) as

$$\bar{T}_i^{\text{QW}} = \frac{\varepsilon_i^o}{k_B}, \quad i = c, v. \quad (26)$$

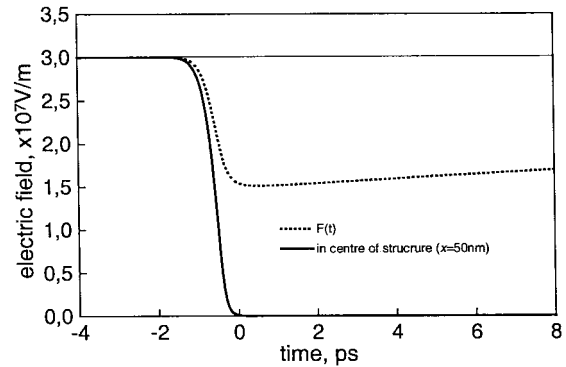
In calculating the curves A(2D) and B(2D), we used (4) with Fermi levels evaluated for a QW and assumed that its thickness is 10 nm. The temperatures \bar{T}_c^{QW} and \bar{T}_v^{QW} have been calculated for the same values for ε_c^o and ε_v^o as in the above case of a bulk absorber, so $\bar{T}_c^{\text{QW}} = 97$ K and $\bar{T}_v^{\text{QW}} = 19$ K. From Fig. 4, we see that the difference between A(2D) and B(2D) is not as large as between curves A(bulk) and B(bulk). This is due to the fact that the temperature \bar{T}_c^{QW} (\bar{T}_v^{QW}) is larger than \bar{T}_c^{bulk} (\bar{T}_v^{bulk}): in QW's, the pump energy ε_c^o (ε_v^o) is spent only for two degrees of freedom, compared to three degrees in the bulk case. Comparing curves A and B in Fig. 4, one can conclude that the fast saturation due to carrier cooling in the QW case will not be so pronounced as in the bulk case [see Fig. 2(b)]. This implies that if mode-locking is based on fast saturation (as in solid-state lasers [20], [21]) the use of bulk saturable absorbers might well be preferable to QW absorbers.

The approximate expressions (18) and (24) can be used in order to derive an equation for the pulse energy

$$E(z) = \hbar\omega_o v_g A_g \int_{-\infty}^{+\infty} dt \cdot S(z, t). \quad (27)$$



(a)



(b)

Fig. 5. (a) Calculated electron temperature dynamics for bulk absorber with different initial electric fields: curve 0 for $F_o = 0$; curve 1 for $F_o = 1 \times 10^7$ V/m; curve 2 for $F_o = 3 \times 10^7$ V/m; curve 3 for $F_o = 5 \times 10^7$ V/m. (b) Dynamics of the electric field in the middle of structure (solid curve), and of the external field F (dotted curve). Input pulse duration $\tau_{in} = 1$ ps and input pulse energy $E_{in} = 20$ pJ.

By integrating (1) over time, using (6) with (18) or (24), and neglecting carrier relaxation terms in (6), we get

$$\frac{dE}{dz} = -\Gamma E_{\text{sat}} \alpha_o [1 - \exp(-E/E_{\text{sat}})] \quad (28)$$

where the saturation energy parameter

$$E_{\text{sat}} = \begin{cases} \frac{\hbar\omega_o A_g}{\alpha_{nB}}, & \tau_{in} \ll \tau_{uc}, \tau_{uv} \\ \frac{\hbar\omega_o A_g}{\alpha_{nA}}, & \tau_{uc}, \tau_{uv} \ll \tau_{in} \ll \tau_S. \end{cases} \quad (29)$$

In the two limit cases of very short and relatively long pulses, the ordinary differential equation (28) can be used instead of the full model [(1), (6)–(7)] to calculate the saturation curves in Fig. 3.

B. Electric Field Effects: Carrier Heating

In this section, we consider the effect on absorption dynamics and pulse propagation of a nonzero initial electric field ($F_o \neq 0$) in a bulk absorbing region. Before the arrival of the optical pulse, there are very few carriers in the absorbing region; any carriers that are there are in equilibrium with the lattice, with a temperature of 300 K. Carriers generated by the pulse are heated by the field and reach temperatures of ~ 1000 K depending on the value of F_o [see Fig. 5(a) in

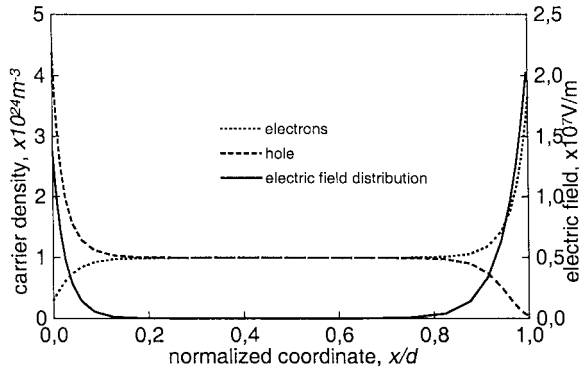
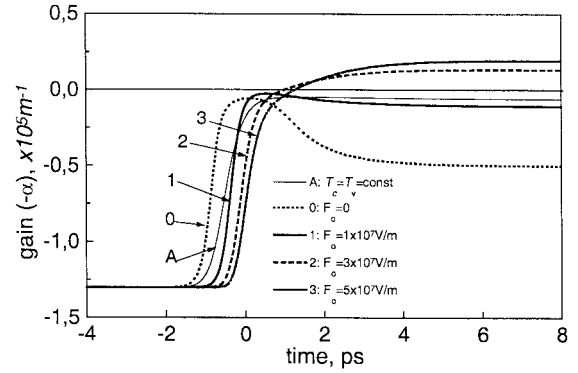


Fig. 6. Distribution of electrons (dotted curve), holes (dashed curve), and of the electric field across the absorbing region after the pulse.

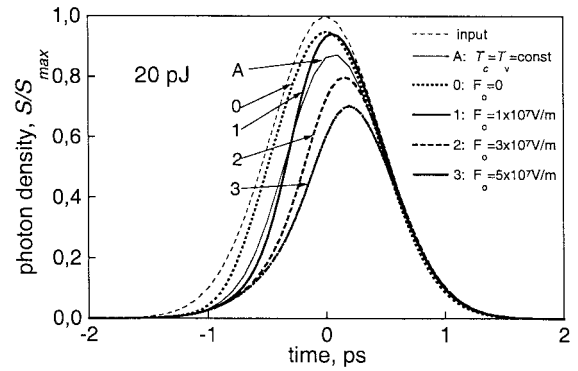
which electron temperature dynamics are shown; behavior of hole temperature is similar]. Accumulation of photogenerated carriers and their redistribution over the absorbing region (electrons are collected near $x = d$, holes near $x = 0$) leads to screening of the electric field inside the structure. Fig. 6 demonstrates an example of such carrier and field distributions. The solid curve in Fig. 5(b) shows the time behavior of the electric field in the middle of the absorbing region. We see that screening of the electric field takes place already at the front of the pulse. High carrier temperatures lead, in particular, to effective thermionic emission and tunneling of carriers from the absorbing region, to partial neutralization of ionized impurities Q_- and Q_+ , and to a corresponding decrease of the field F [see dotted curve in Fig. 5(b)]. After the pulse passes through the device, the field recovers to its initial value F_o .

After increasing, the carrier temperatures decrease [see Fig. 5(a)]. This behavior is caused by weakening of carrier heating by the electric field due to screening of the field [Fig. 5(b)] and by effective carrier cooling. Two mechanisms contribute to the cooling. The first one is carrier-phonon scattering, which leads to cooling of hot carriers to the lattice temperature. The second mechanism is generation of cold carriers by the pulse. As discussed in Section III-A, the pulse generates cold electrons and holes near the edges of the conduction and valence bands with energies ε_c^o and ε_v^o . Previously generated hot carriers share their energy with the cold carriers, leading to very effective cooling of carriers in the absorbing region.

The temperature dynamics define the behavior of absorption and pulse shaping. Fig. 7(a) shows the gain dynamics (the gain $g = -\alpha$) at different initial electric fields F_o , and Fig. 7(b) shows the corresponding output pulses together with the input pulse ($\tau_{in} = 1$ ps, $E_{in} = 20$ pJ). For comparison, curves A describe the case when temperature dynamics are ignored. We see that application of a nonzero field and the resulting carrier heating leads to suppression of saturation (curves 1–3) during the initial stage of absorption, in comparison with the case when temperature dynamics are ignored (curve A), and the case of zero electric field (curve 0). Accordingly, the absorption of the front of the pulse is much stronger (curves 1–3 versus curves A and 0). Generation of carriers, electric field screening, and carrier cooling lead, finally, to a fast transition from unsaturated absorption to strongly saturated



(a)



(b)

Fig. 7. (a) Gain ($-\alpha$) dynamics and (b) output pulses for different initial fields F_o . Curves 0–3 are for the same conditions as in Fig. 5. Curve A is calculated for $T_c = T_v = 300$ K. The thin dashed curve in (b) is the input pulse. Input pulse duration $\tau_{in} = 1$ ps and input pulse energy $E_{in} = 20$ pJ.

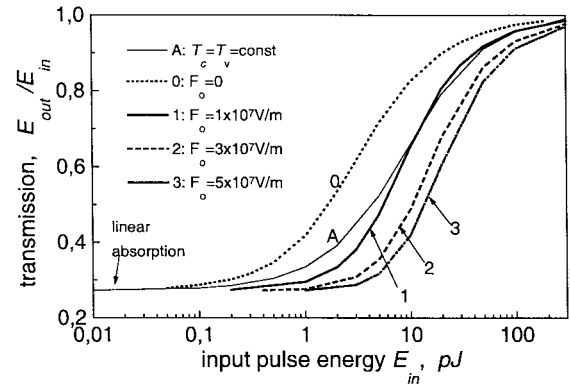


Fig. 8. Calculated dependence of transmission E_{out}/E_{in} of an input pulse energy E_{in} for different initial electric fields F_o . Notations for curves are the same as for Figs. 5 and 7. Input pulse duration $\tau_{in} = 1$ ps.

absorption. The moment of the transition (i.e., the saturation time delay) depends on the initial field F_o . For larger F_o , the carrier heating in the initial stages of absorption is stronger, and more carriers must be generated to screen the field in order to achieve substantial carrier cooling and to saturate absorption. Thus the transition occurs at later times for larger initial fields [curves 1–3 in Fig. 7(a)]. In other words, the larger the field, the larger the pulse energy needed to saturate the absorption. Fig. 8 shows saturation curves (dependence of the transmission, E_{out}/E_{in} , on the input pulse energy E_{in}) for

different fields F_o . We see that the saturation curves strongly depend on the applied field F_o . For instance, in order to saturate absorption in the case $F_o = 5 \times 10^7$ V/m (curve 3 in Fig. 8), the input pulse energy E_{in} must be an order of magnitude larger than in the case of zero field (curve 0). Thus, the saturation energy in the absorbing medium depends on the electric field F_o which in turn depends on the applied bias voltage—an externally controllable parameter.

From Fig. 7(b), we see that the application of the electric field F_o leads to stronger pulse shortening in comparison with the case of zero electric field (curves 1–3 versus curve 0) for $E_{in} = 20$ pJ. Obviously, larger electric fields should be applied in order to shorten higher energy pulses. This effect of improved pulse shaping with applied electric field in bulk absorbers could be used in passively mode-locked and Q-switched lasers for generation of high-energy picosecond pulses.

If a sufficient carrier density is generated during the period of unsaturated absorption, positive gain can be obtained after carrier cooling [curves 2–3 in Fig. 7(a)]. Thus, in absorbers with applied or built-in electric fields, a transition from absorption to gain can be achieved. In the case of $E_{in} = 20$ pJ, the gain conditions are reached after the pulse leaves the absorber so the pulse does not feel the gain. However, after reflection by a mirror, the shortened output pulse can make a return pass through the device when gain is present, and thus be amplified [36]. In this case, pulse shortening can be achieved with smaller losses of pulse energy. This configuration, with the pulse experiencing gain on its return trip through the absorber, could be useful in mode-locked and Q-switched lasers, particularly monolithic mode-locked semiconductor lasers.

IV. SUMMARY AND CONCLUSION

We have considered the effects of carrier cooling and carrier heating on saturation and pulse shaping in bulk semiconductor waveguide absorbers. Carrier cooling takes place in the case of zero electric field in the absorber and leads to strong additional fast saturation in comparison with the case when temperature changes are ignored. The additional saturation disappears on a picosecond time scale, together with the relaxation of the carriers to the lattice temperature. The fast saturation also takes place in QW absorbers and can be responsible for mode-locking in solid-state and mode-locked diode lasers with QW saturable absorbers. In diode lasers with QW absorbers, the electric field does not heat the photogenerated carriers due to carrier confinement in the QW in the direction of the field, so in this case carrier cooling also takes place. Comparing carrier cooling in bulk and QW absorbers, we found that in bulk absorbers the cooling is stronger, and accordingly, the fast saturation is larger. It implies that bulk absorbers may be preferable for use in solid-state mode-locked lasers. The additional saturation due to carrier cooling leads to a dependence of saturation energy on pulse duration, the saturation energy decreasing with the pulse duration. These decreased saturation energies can restrict the pulse energies that can be generated by mode-locked lasers.

Applying a nonzero electric field to a bulk semiconductor absorber leads to carrier heating by the field. Accordingly, saturation of absorption is suppressed in comparison with the case of zero electric field. Transition from unsaturated absorption to saturated occurs only as result of screening of the electric field by photogenerated carriers. As the electric field is screened, carriers in the absorber are cooled due to carrier–phonon interaction and by cold carriers generated by the pulse. Due to the mechanisms of saturation via field screening and carrier cooling, the duration of the transition from unsaturated absorption to strong saturation and even to gain (if enough carriers are generated during the stage of suppressed saturation) is defined by intraband carrier kinetics times and can be on picosecond and subpicosecond time scales.

This carrier heating by the electric field leads to a dependence of saturation energy on the electric field: the saturation energy increases strongly with the field. Accordingly, higher energy pulses can be shortened with a bulk saturable absorber by externally increasing the applied reverse bias, without increasing the absorber length. This external control of pulse shaping could be useful for obtaining high energy pulses in mode-locked and Q-switched semiconductor lasers.

Finally, it has been discussed already [38], [39] that bulk absorbing regions can be preferable to QW's for use as saturable absorbers in mode-locking. The model presented in this paper shows that carrier temperature dynamics in bulk absorbers offer some additional opportunities in comparison with QW absorbers for controlling saturation dynamics, pulse saturation energies, and pulse shortening, and could be useful for generating high-energy picosecond optical pulses.

REFERENCES

- [1] K. L. Hall, J. Mark, E. P. Ippen, and G. Eisenstein, "Femtosecond gain dynamics in InGaAsP optical amplifiers," *Appl. Phys. Lett.*, vol. 56, pp. 1740–1742, 1990.
- [2] B. N. Gommatam and A. P. DeFonzo, "Theory of hot carriers effects on nonlinear gain in GaAs/GaAlAs lasers and amplifiers," *IEEE J. Quantum Electron.*, vol. 26, pp. 1689–1704, 1990.
- [3] M. Willatzen, A. Uskov, J. Mørk, H. Olesen, B. Tromborg, and A.-P. Jauho, "Nonlinear gain suppression in semiconductor lasers due to carrier heating," *IEEE Photon. Technol. Lett.*, vol. 3, pp. 606–609, 1991.
- [4] J. Mark and J. Mørk, "Subpicosecond gain dynamics in InGaAsP optical amplifiers: Experiment and theory," *Appl. Phys. Lett.*, vol. 61, pp. 2281–2283, 1992.
- [5] Y. Lai, K. L. Hall, E. P. Ippen, and G. Eisenstein, "Short pulse gain saturation in InGaAsP diode laser amplifiers," *IEEE Photon. Technol. Lett.*, vol. 2, pp. 711–713, 1990.
- [6] K. L. Hall, Y. Lai, E. P. Ippen, G. Eisenstein, and U. Koren, "Femtosecond gain dynamics and saturation behavior in well optical amplifiers," *Appl. Phys. Lett.*, vol. 57, pp. 2888–2890, 1990.
- [7] A. Uskov, J. Mørk, and J. Mark, "Theory of short pulse gain saturation in semiconductor laser amplifiers," *IEEE Photon. Technol. Lett.*, vol. 4, pp. 443–446, 1992.
- [8] M. Y. Hong, Y. H. Chang, A. Dienes, J. P. Heritages, and P. J. Delfyett, "Subpicosecond pulse amplification in semiconductor laser amplifier: Theory and experiment," *IEEE J. Quantum Electron.*, vol. 30, pp. 1122–1131, 1994.
- [9] Y. Nambu and A. Tomita, "Spectral hole-burning and carrier heating effects on the transient optical nonlinearity of highly carrier-injected semiconductor," *IEEE J. Quantum Electron.*, vol. 30, pp. 1981–1999, 1994.
- [10] V. Tolstikhin and M. Willander, "Carrier heating effects in dynamic-single-frequency GaInAsP–InP laser diodes," *IEEE J. Quantum Electron.*, vol. 31, pp. 814–833, 1995.

- [11] J. Mørk and A. Mecozzi, "Theory of the ultrafast optical response of active semiconductor waveguides," *J. Opt. Soc. Amer., B*, vol. 13, pp. 1803–1815, 1996.
- [12] J. A. Tatum, D. L. MacFarlane, R. C. Bowen, G. Klimeck, and W. R. Frensley, "Ultrafast characteristics of InGaP–InGaAlP laser amplifiers," *IEEE J. Quantum Electron.*, vol. 32, pp. 664–669, 1996.
- [13] C. Y. Tsai, C. Y. Tsai, R. M. Spencer, Y.-H. Lo, and L. F. Eastman, "Nonlinear gain coefficients in semiconductor lasers: Effects of carrier heating," *IEEE J. Quantum Electron.*, vol. 32, pp. 201–212, 1996.
- [14] R. A. Indik, R. Binder, M. Mlejnek, J. V. Moloney, S. Hughes, A. Knorr, and S. W. Koch, "Role of plasma cooling, heating, and memory effects in subpicosecond pulse propagation in semiconductor amplifiers," *Phys. Rev. A*, vol. 53, pp. 3614–3620, 1996.
- [15] J. Wang and H. Schweizer, "A quantitative comparison of the classical rate-equation model with the carrier heating model on dynamics of the quantum-well laser: The role of carrier energy relaxation, electron-hole interaction, and Auger effect," *IEEE J. Quantum Electron.*, vol. 33, pp. 1350–1359, 1997.
- [16] D. J. Derickson, R. J. Helkey, A. Mar, J. Karin, J. G. Wasserbauer, and J. E. Bowers, "Short pulse generation using multisegment mode-locked semiconductor lasers," *IEEE J. Quantum Electron.*, vol. 28, pp. 2186–2201, 1992.
- [17] Y.-K. Chen and M. C. Wu, "Monolithic colliding-pulse mode-locked quantum-well lasers," *IEEE J. Quantum Electron.*, vol. 28, pp. 2176–2185, 1992.
- [18] P. P. Vasil'ev, "High-power high-frequency picosecond pulse generation by passively *Q*-switched 1.55 μm diode lasers," *IEEE J. Quantum Electron.*, vol. 29, pp. 1687–1692, 1993.
- [19] J. F. Martins-Filho, E. A. Avrutin, C. N. Ironside, and J. L. Roberts, "Monolithic multiple colliding pulse modelocking quantum well lasers," *IEEE J. Select. Topics Quantum Electron.*, vol. 1, pp. 539–551, 1995.
- [20] U. Keller, K. J. Weingarten, F. X. Kartner, D. Kopf, B. Braun, I. D. Jung, R. Fluck, C. Honninger, N. Matuschek, and J. Aus der Au, "Semiconductor saturable absorber mirrors (SESAM's) for femtosecond to nanosecond pulse generation in solid-state lasers," *IEEE J. Select. Topics Quantum Electron.*, vol. 2, pp. 435–453, 1996.
- [21] S. Tsuda, W. H. Knox, S. T. Cundiff, W. Y. Jan, and J. E. Cunningham, "Mode-locking ultrafast solid-state lasers with saturable Bragg reflectors," *IEEE J. Select. Topics Quantum Electron.*, vol. 2, pp. 454–464, 1996.
- [22] S. Bischoff, M. P. Sorensen, J. Mørk, S. D. Brorson, T. Franck, J. M. Nielsen, and A. Moller-Larsen, "Pulse-shaping mechanism in colliding-pulse mode-locked lasers diodes," *Appl. Phys. Lett.*, vol. 67, pp. 3877–3879, 1995.
- [23] S. Bischoff, J. Mørk, T. Franck, S. D. Brorson, M. Hofmann, K. Frojdh, L. Plip, and M. P. Sorensen, "Monolithic colliding pulse mode-locked semiconductor lasers," *Quantum Semiclass. Opt.*, vol. 9, pp. 655–674, 1997.
- [24] J. R. Karin, R. Helkey, D. Derickson, R. Nagarajan, D. Allin, J. Bowers, and R. Thornton, "Ultrafast dynamics in field-enhanced saturable absorbers," *Appl. Phys. Lett.*, vol. 64, pp. 676–678, 1994.
- [25] J. R. Karin, A. V. Uskov, R. Nagarajan, J. E. Bowers, and J. Mørk, "Carrier heating dynamics in semiconductor waveguide saturable absorbers," *Appl. Phys. Lett.*, vol. 65, pp. 2708–2711, 1994.
- [26] A. V. Uskov, J. R. Karin, R. Nagarajan, and J. E. Bowers, "Dynamics of carrier heating and sweepout in waveguide saturable absorbers," *IEEE J. Select. Topics Quantum Electron.*, vol. 1, pp. 552–561, 1995.
- [27] S. D. Brorson, S. Bischoff, J. Mørk, A. Moeller-Larsen, and J. M. Nielsen, "Femtosecond carrier dynamics and modelocking in monolithic CPM lasers," *IEEE Photon. Technol. Lett.*, vol. 7, pp. 1148–1151, 1995.
- [28] M. Hofmann, K. Frojdh, S. D. Brorson, and J. Mørk, "Temporal and spectral dynamics in multi-quantum-well semiconductor saturable absorbers," *IEEE Photon. Technol. Lett.*, vol. 9, pp. 622–624, 1997.
- [29] S. Gee, R. Coffie, P. J. Delfyett, G. Alphonse, and J. Connolly, "Intracavity gain and absorption dynamics of hybrid modelocked semiconductor lasers using multiple quantum well saturable absorbers," *Appl. Phys. Lett.*, vol. 71, pp. 2369–2371, 1997.
- [30] A. Uskov, J. Karin, J. E. Bowers, and J. G. McInerney, "Intraband carrier kinetics and picosecond pulse shaping in field-enhanced absorber," *Opt. Lett.*, vol. 23, pp. 376–379, 1998.
- [31] G. P. Agrawal, "Effect of gain dispersion on ultrashort pulse amplification in semiconductor laser amplifiers," *IEEE J. Quantum Electron.*, vol. 27, pp. 1843–1849, 1991.
- [32] S. M. Sze, *Physics of Semiconductor Devices*, 2nd ed. New York: Wiley-Interscience, 1981.
- [33] A. Yariv, *Optical Electronics in Modern Communications*, 5th ed. New York: Oxford, 1996.
- [34] C.-Y. Tsai, C.-Y. Tsai, Yu-H. Lo, and L. F. Eastman, "Carrier energy relaxation time in quantum-well lasers," *IEEE J. Quantum Electron.*, vol. 31, pp. 2148–2158, 1995.
- [35] L. Landau and E. Lifshitz, *Quantum Mechanics*. New York: Addison-Wesley, 1958.
- [36] G. P. Agrawal and N. A. Olsson, "Self-phase modulation and spectral broadening of optical pulses in semiconductor laser amplifiers," *IEEE J. Quantum Electron.*, vol. 25, pp. 2297–2306, 1989.
- [37] J. R. Karin, "Ultrafast dynamics in semiconductor laser structures," Ph.D. dissertation, Univ. of California at Santa Barbara, 1994.
- [38] J. A. Leegwater, "Theory of mode-locked semiconductor lasers," *IEEE J. Quantum Electron.*, vol. 32, pp. 1782–1792, 1996.
- [39] R. G. M. P. Koumans, R. van Roijen, B. H. Verbeek, M. B. van der Mark, and C. T. H. F. Liedenbaum, "Ultra-short pulse generation at 1.3 μm by an integrated colliding pulse mode-locked laser using all bulk material," presented at the Optical Fiber Conf., San Diego, CA, Feb. 1995.

Alexander V. Uskov (M'97), photograph and biography not available at the time of publication.

J. R. Karin, photograph and biography not available at the time of publication.

John E. Bowers (S'78–M'81–SM'85–F'93), photograph and biography not available at the time of publication.

John G. McInerney (M'81), photograph and biography not available at the time of publication.

Jean Le Bihan (M'94–SM'95), photograph and biography not available at the time of publication.